Applied Surface Science 567 (2021) 150836

Contents lists available at ScienceDirect

Applied Surface Science

journal homepage: www.elsevier.com/locate/apsusc

Full Length Article

Performance of toluene oxidation over MnCe/HZSM-5 catalyst with the addition of NO and NH_3

Peng Lu [a,b], Lyumeng Ye [c], Xianhui Yan [a,b], Dingsheng Chen [a,b], Dongyao Chen [a,b], Xiongbo Chen [a,b], Ping Fang [a,b], Chaoping Cen [a,b,*]

[a] Guangdong Province Engineering Laboratory for Air Pollution Control, South China Institute of Environmental Sciences, MEE, Guangzhou 510655, China
[b] Guangdong Provincial Key Laboratory of Water and Air Pollution Control, Guangzhou 510655, China
[c] School of Environmental Science and Engineering, Sun Yat-sen University, Guangzhou 510275, China

ARTICLE INFO

Keywords:
Toluene oxidation
NH_3-SCR
Byproducts
MnCe/HZSM-5 catalyst
In-situ DRIFTs

ABSTRACT

Toluene and NO_x can be co-removed in NH_3-SCR unit. The evaluation of toluene oxidation performance with the participation of SCR reactants is momentous but lacking. Herein, a MnCe/HZSM-5 catalyst was prepared to investigate the effects of NO and NH_3 on toluene oxidation. The addition of NO and NH_3 increased the toluene conversion from 76.6% to 91.8%, but decreased the CO_2 selectivity from 60.5% to 34.1% at 250 °C, indicating that more carbon was transferred into the byproducts. NO and NH_3 participated in toluene oxidation by reacting with intermediates, such as aldehydes, carboxylic acids or phenol, to form nitriles or nitrobenzene. Most of nitriles and nitrobenzene were in solid byproducts, which deposited on catalyst surface and deactivated the catalyst. SCR reactants accelerated the decrease of Mn^{4+}, Ce^{3+}, O_{sur} proportions and Lewis acid sites, which were the active constituents for toluene oxidation. As a consequence, a faster deactivation occurred. NO was competitively adsorbed on catalyst with toluene, but promoted toluene oxidation. On the contrary, NH_3 enhanced toluene adsorption, but inhibited toluene oxidation. The *in-situ* DRIFTs results showed that NO and NH_3 inhibited the deep oxidation of toluene based on the observation of less water, carboxylate and carbonate.

1. Introduction

As the common precursors of tropospheric ozone and secondary organic aerosol, volatile organic compounds (VOCs) and nitrogen oxides (NO_x) urgently need to be well controlled [1]. The Chinese government proposed a 10% reduction of VOCs and NO_x emission during the 14th five-year plan period (2021–2025). VOCs and NO_x will be emitted together in some industries, such as solid waste incineration, iron ore sintering and metal smelting [2]. Recently, simultaneous removal of VOCs in current existing NH_3-SCR unit has drawn considerable interest due to the advantage of cost and land use saving [3–8]. The similar redox property requirement of catalyst and active temperature window make this technology possible. Nevertheless, the rational design of effective dual functional catalysts relies on the understanding of collaborative removal mechanism, which remains challenging.

The commercial V_2O_5-$WO_3(MoO_3)/TiO_2$ SCR catalysts have been explored for the co-removal of VOCs and NO_x [2,3,5]. Huang et al. [3] observed the V_5Mo_5Ti catalyst exhibited 100% NO conversion above 200 °C. The chlorobenzene (CB) conversion reached ~60% requiring a higher temperature than ~270 °C. By adding noble metal Pd, Li et al. [5] synthesized a PdV/TiO_2 catalyst for the co-removal of CB and NO_x. The catalyst showed excellent NO conversion. The temperature still needed to be ~300 °C to give a ~80% CB conversion. Alternatively, some researchers adopted the Mn-based catalysts to eliminate VOCs and NO_x in relatively lower temperature window [7,9]. In our previous works [10,11], HZSM-5 modified MnO_x-CeO_2 (MnCe/HZSM-5) catalyst and MnFe spinel catalyst were prepared and delivered acceptable performance for simultaneous removal of toluene and NO_x. The impacts of toluene on NH_3-SCR reaction were revealed. Briefly, toluene inhibited NO conversion and byproduct N_2O formation.

It's worth noting that NH_3-SCR reactants affect the VOCs oxidation during simultaneous removal process as well, causing some desirable or undesirable consequences. The adsorption of reactants is the first step in heterogeneous catalysis. Some researchers observed the competitive adsorption between VOCs and NO/NH_3. Huang et al. [12] found NH_3 could be competitively adsorbed on acid sites of catalyst with CB,

* Corresponding author at: South China Institute of Environmental Sciences, MEE, Guangzhou 510655, China.
E-mail address: cenchaoping@scies.org (C. Cen).

https://doi.org/10.1016/j.apsusc.2021.150836
Received 20 June 2021; Received in revised form 25 July 2021; Accepted 1 August 2021
Available online 5 August 2021

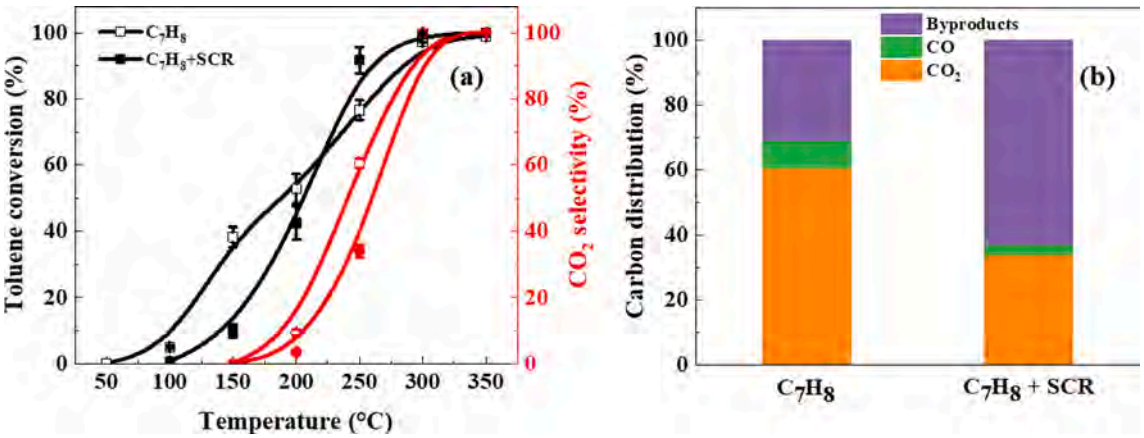

Fig. 1. (a) Toluene conversion and CO_2 selectivity and (b) carbon distribution in products at 250 °C. Reaction conditions: [C_7H_8] = 50 ppm, [NO] = [NH_3] = 500 ppm (when used), [O_2] = 10 vol%, Q = 200 mL/min, GHSV = 60,000 mL/(g·h).

inhibiting the adsorption and activation of CB. Martinovic et al. [13] believed NO and VOCs were adsorbed on the same metal sites resulting in the competition for the same redox sites. As for the activation of reactants, VOCs oxidation will be promoted by NO_x resulted from the strong oxidizing ability of NO_2 which accelerates the re-oxidation of reduced metal sites [14]. But this promotional effect can only be observed under certain conditions, such as in the presence of oxygen [6] or to be present as adsorbed NO_2 instead of nitrate species [1]. NO/NH_3 may participate in the VOCs oxidation due to the detection of byproducts such as benzonitrile, aniline and nitrobenzene [2,15], which deposited on catalyst surface as coke and deactivated the catalyst. However, the effects of SCR reactants on VOCs oxidation have not reached a common view yet. For instance, Zhao et al. [16] found SCR reactants enhanced the toluene oxidation over $CuCeAl_x$ catalyst because NO acted as the oxidizing agent of toluene. But Ye et al. [1] observed a negative effect over MnO_x-CeO_2 catalyst due to the competitive adsorption of toluene and NH_3 and the poisoned byproduct nitriles. In conclusion, there are some uncertainties needed to be well addressed in the future: (1) the co-adsorption behavior of reactants (VOCs, NO and NH_3); (2) the effect of NO and NH_3 on the activation and deep oxidation of VOCs; (3) the migration and transformation of C and N during simultaneous removal process.

MnCe/HZSM-5 has been proved to be a good choice for simultaneous removal of toluene and NO_x due to variable valence states of metals, high redox ability, abundant acid sites and large surface area [17–22]. In this work, MnCe/HZSM-5 catalyst was used for the simultaneous removal of toluene and NO_x. Special attention has been paid to the effect of NH_3-SCR reactants (NO and NH_3) on toluene oxidation. Performance testing, gas chromatography coupled with a mass spectrometer (GC–MS), temperature programmed desorption of NH_3 (NH_3-TPD) and *in-situ* diffuse reflectance infrared Fourier transforms (DRIFTs) were conducted to investigate the toluene catalytic oxidation activity and the reaction mechanism. Characterizations such as thermogravimetric analysis (TGA), surface deposition-temperature programmed desorption (SD-TPD), X-ray photoelectron spectroscopy (XPS) and pyridine adsorbed IR spectroscopy (Py-IR) were carried out to reveal the impacts on catalysts properties and to support the mechanism discussion.

2. Experimental section

2.1. Catalyst preparation

The molar ratio of Mn and Ce in catalyst was 1:1. The mass ratio of HZSM-5 support with a SiO_2/Al_2O_3 ratio of 25 was 80%. Detailed preparation method of MnCe/HZSM-5 catalyst can be found in previous work [11].

2.2. Catalytic activity measurement

Toluene catalytic oxidation was carried out in a lab-scale fixed-bed quartz tube (i.d. = 8 mm) reactor at 50–350 °C. 200 mL/min feed gas passed through 0.2 g catalyst with a gas hourly space velocity (GHSV) of 60,000 mL/(g h). The composition of feed gas was 50 ppm C_7H_8, 500 ppm NH_3 (when used), 500 ppm NO (when used), 10 vol% O_2 and balance of N_2. The inlet and outlet gases were monitored by an on-line FTIR spectrometer (GASMET DX-4000). The toluene conversion and CO_2 selectivity were obtained by Eqs. (1)–(2).

$$Toluene\ conversion\ (\%) = \frac{C^{in}_{toluene} - C^{out}_{toluene}}{C^{in}_{toluene}} \times 100\% \quad (1)$$

$$CO_2\ selectivity\ (\%) = \frac{C_{CO2}}{7\left(C^{in}_{toluene} - C^{out}_{toluene}\right)} \times 100\% \quad (2)$$

The gaseous byproducts were identified by a GC–MS system (Agilent 6890N GC-5975B MSD). The solid byproducts were detected by a thermal desorption instrument (APL-TD-2) coupled with GC–MS. ~0.1 g sample was purged in He at 30 °C for 2 min, then heated to 300 °C and held for 3 min to desorb. The desorbed species were collected in a cold trap, which was then rapidly heated to 300 °C to release the organic species into the GC–MS. The initial GC oven temperature was 35 °C for 10 min, then increased to 150 °C with a rate of 5 °C/min and held for 7 min, finally increased to 200 °C with a rate of 10 °C/min and held for 4 min. The quadrupole and ion source temperatures were 150 °C and 230 °C, respectively.

2.3. Catalyst characterization

Temperature programmed desorption (TPD) was conducted by an on-line FTIR spectrometer (GASMET DX-4000). The SD-TPD was carried out by the same instrument. ~0.1 g sample was placed in a fixed-bed quartz reactor. The sample was preheated in N_2 at 350 °C for 1 h, then cooled down to 50 °C. Next, the sample was exposed to the experimental atmosphere for 3 h at 250 °C, then cooled down to 50 °C. Finally, the sample was heated to 600 °C with a rate of 10 °C/min in 100 mL/min 10 vol% O_2 (balance of N_2) to record the TPD profile.

XPS was carried out by Thermo Scientific ESCALAB 250 with Al Kα X-ray radiation (1486.6 eV) operated at 150 W. A DSC/DTA-TG instrument (STA 449 F3 Jupiter, NETZSCH) was applied to conduct the TGA. ~10 mg sample was heated in air to 800 °C with a rate of 10 °C/min. Py-IR experiments were conducted using an FTIR spectrometer (PerkinElmer). ~0.05 g sample was pretreated in a vacuum at 350 °C for 2 h, followed by adsorption of pyridine at room temperature for 0.5 h. The sample was then heated to 200 °C/350 °C and maintained for 1 h to

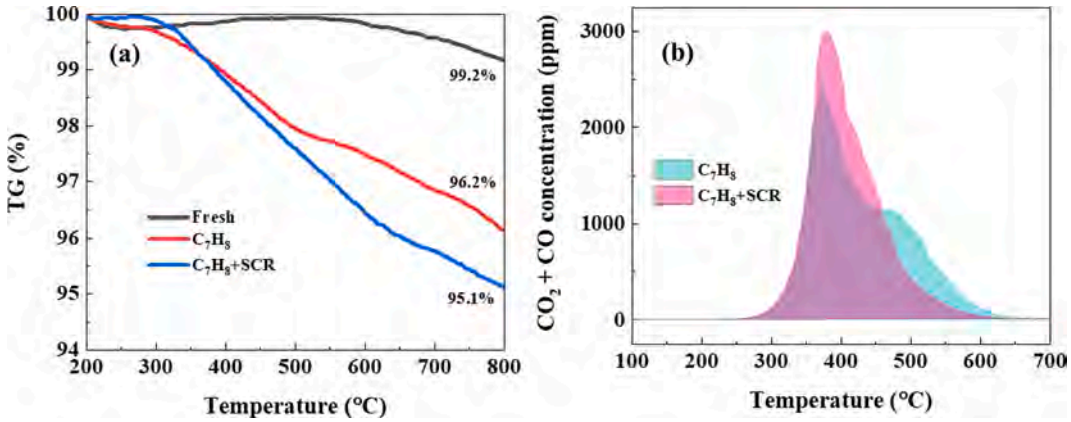

Fig. 2. (a) TG and (b) SD-TPD results of used catalysts after reaction at 250 °C.

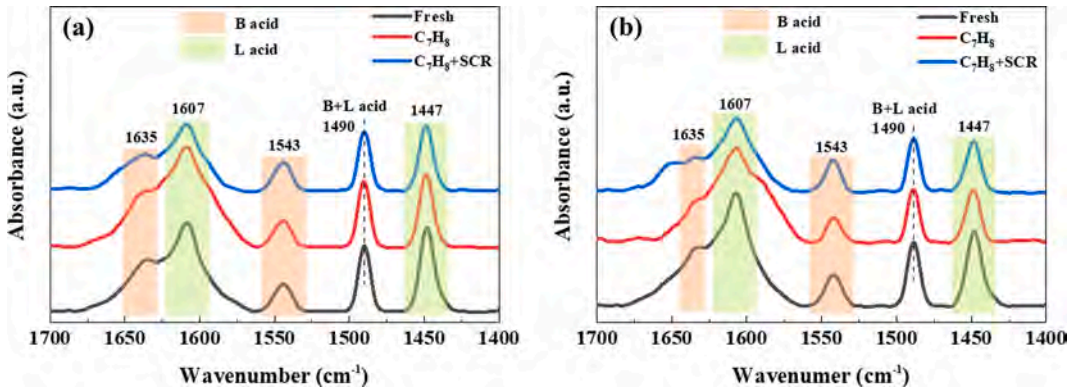

Fig. 3. Py-IR spectra of used catalysts after desorption of pyridine at (a) 200 °C and (b) 350 °C.

desorb pyridine. The Py-IR spectra were recorded at a resolution of 1 cm^{-1}. A FTIR spectrometer (Bruker VERTEX 70) equipped with IR cell, KBr windows and MCT detector was used to perform the *in-situ* DRIFTs experiments. The sample was pretreated in N_2 at 350 °C for 1 h, then cooled down to the experimental temperature. The sample was exposed to reaction atmosphere and the spectra were recorded by accumulating 64 scans with a resolution of 4 cm^{-1}.

3. Results and discussion

3.1. Toluene oxidation performance

The T_{50} and T_{90} (the temperatures at which the toluene conversions were 50% and 90%) of MnCe/HZSM-5 catalyst were 189.6 °C and 282.3 °C, respectively (Fig. 1a). When NH_3-SCR reactants (NO and NH_3) were added, the T_{50} increased to 207.6 °C and the T_{90} decreased to 248.2 °C. NO and NH_3 addition enhanced the toluene conversion at temperatures higher than ~225 °C. Meanwhile, the NO and NH_3 conversions were higher than 72% and 96% above 200 °C with a stable N_2 selectivity > 94% (Fig. S1). These results suggested that toluene and NO could be effectively co-removed over MnCe/HZSM-5 catalyst. However, the CO_2 selectivity was remarkably decreased, which suggested that more byproducts were generated. The carbon distribution after toluene oxidation at 250 °C was summarized in Fig. 1b. The proportions of CO_2 and CO decreased from 60.5% and 8.5% to 34.1% and 3.0%, respectively. As a consequence, the byproduct proportion increased significantly to 62.9%, leading to an unavoidable deactivation of catalyst (Fig. S2a). When temperature reached 300 °C, nearly all toluene was completely oxidized to CO_2, and the influence of SCR reactants was ignorable. The catalytic activity maintained in the long-term experiments for 16 h at 300 °C (Fig. S2b).

3.2. Used catalyst characterization

The used catalysts after reactions at 250 °C were characterized by TG and SD-TPD. Only ~0.8% weight loss was recorded for the fresh catalyst (Fig. 2a). After toluene oxidation, the weight loss of catalyst increased to ~3.8% resulted from the deposited solid byproducts. A more significant weight loss of ~4.9% was observed with the addition of NO and NH_3 due to more solid byproducts generated. The SD-TPD results also proved this

Table 1
Information obtained from XPS spectra and Py-IR spectra of used catalysts.

Sample	Py-IR results* (200 °C)		Py-IR results* (350 °C)		XPS results		
	B acid sites (mmol/g)	L acid sites (mmol/g)	B acid sites (mmol/g)	L acid sites (mmol/g)	Mn^{4+}/Mn (%)	Ce^{3+}/Ce (%)	O_{sur}/O (%)
Fresh catalyst	0.155	0.311	0.116	0.202	34.7	23.0	79.5
C_7H_8-used	0.143	0.251	0.080	0.123	30.8	21.8	79.2
C_7H_8 + SCR-used	0.154	0.223	0.108	0.122	20.1	21.2	77.3

* Amounts of B and L acid sites [20]: C(pyridine on B sites) = $1.88IA(B)R^2/W$ and C(pyridine on L sites) = $1.42IA(L)R^2/W$, Where C = concentration (mmol/g catalyst), IA (B or L) = integrated absorbance of B or L band (cm^{-1}), R = radius of catalyst disk (cm), W = weight of disk (mg).

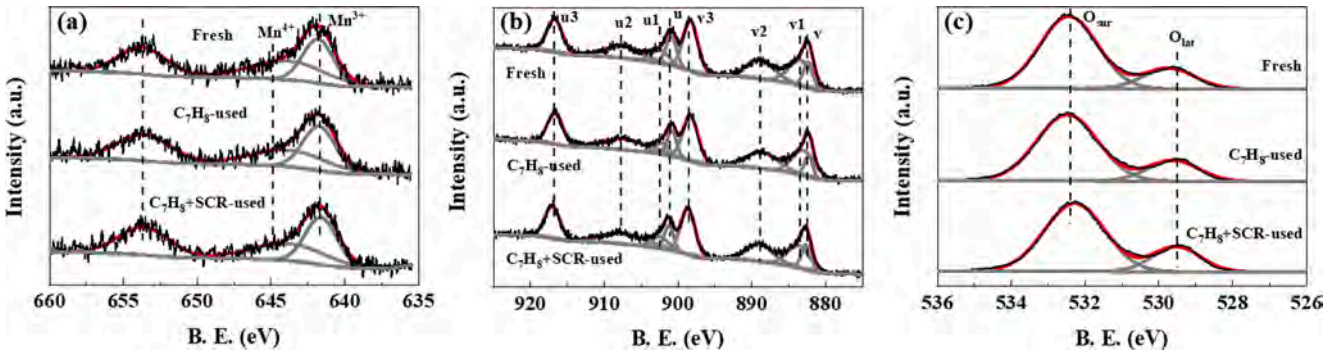

Fig. 4. XPS spectra of (a) Mn 2p, (b) Ce 3d and (c) O 1s.

phenomenon (Fig. 2b). The desorption amount of CO_2 + CO of C_7H_8 + SCR-used catalyst was 1379 μmol/g, which was larger than that of C_7H_8-used catalyst (1340 μmol/g).

The Py-IR spectra of fresh/used catalysts and corresponding data were shown in Fig. 3 and Table 1. The bands at 1635 and 1543 cm^{-1} were assigned to pyridine adsorbed on B acid sites, and the bands at 1607 and 1447 cm^{-1} were corresponded to pyridine adsorbed on L acid sites [23,24] (Fig. 3a). The band at 1490 cm^{-1} was related to B and L acid sites. After toluene oxidation at 250 °C, the amounts of B and L acid sites on catalyst decreased from 0.155 and 0.311 mmol/g to 0.143 and 0.251 mmol/g respectively (Table 1). It was reported that the L acid sites played a core role in C—C band cleavage [20,25]. The consumption of L acid sites may cause the catalyst deactivation. The coke deposition during toluene oxidation will gradually occupy the L acid sites. When SCR reactants were added, the decrease of L acid sites was much more significant, resulting from the occupation of NH_3 and more coke generated. A similar rule was observed for the strong acid sites identified after the desorption of pyridine at 350 °C (Fig. 3b and Table 1).

The fresh/used catalysts were then characterized by XPS for determination of the elemental valance states of Mn, Ce and O. The binding energies at 643.8 eV and 641.6 eV were assigned to Mn^{4+} and Mn^{3+} [26], respectively (Fig. 4a). The Ce 3d spectra were divided into eight bands [16] (Fig. 4b). The bands v1 and u1 represented the $3d^{10}4f^1$ initial electronic state belonging to Ce^{3+}. The others represented the $3d^{10}4f^0$ state corresponding to Ce^{4+}. The redox cycle between Mn^{3+}/Mn^{4+} and Ce^{4+}/Ce^{3+} ($Mn^{3+} + Ce^{4+} \leftrightarrow Mn^{4+} + Ce^{3+}$) notably enhanced the electron transfer and benefited the adsorption/activation of toluene. The O 1s spectra were fitted with two components [7] (Fig. 4c). The bands at 532.3 eV and 529.5 eV corresponded to the surface adsorbed oxygen (O_{sur}, O_2^{2-}, O^- and OH^-) and lattice oxygen (O_{lat}), respectively. A high ratio of Mn^{4+}/Mn has been considered an important factor for good redox capability [26]. The formation of Ce^{3+} creates a charge imbalance, requiring abundant oxygen vacancies to compensate for charge neutrality [16,20]. The ratio of O_{sur} is the barometer to the amounts of oxygen vacancies and surface active oxygen, which play important role in the catalytic oxidation reaction [27–29]. Thus, high concentrations of Mn^{4+}, Ce^{3+} and O_{sur} are beneficial for the catalytic removal of toluene. The used catalysts had lower proportions of Mn^{4+}, Ce^{3+} and O_{sur} (Table 1) compared with fresh catalyst, suggesting the gradual decrease of catalyst activity. The addition of NO and NH_3 may accelerate this deactivation tendency due to larger decrease of Mn^{4+}, Ce^{3+} and O_{sur} proportions.

3.3. Byproducts identification

The solid byproduct composition was analyzed by TD-GC–MS (Fig. S3a and Table S1). The main components of solid byproducts after toluene oxidation were benzene, benzaldehyde and p-xylene. The

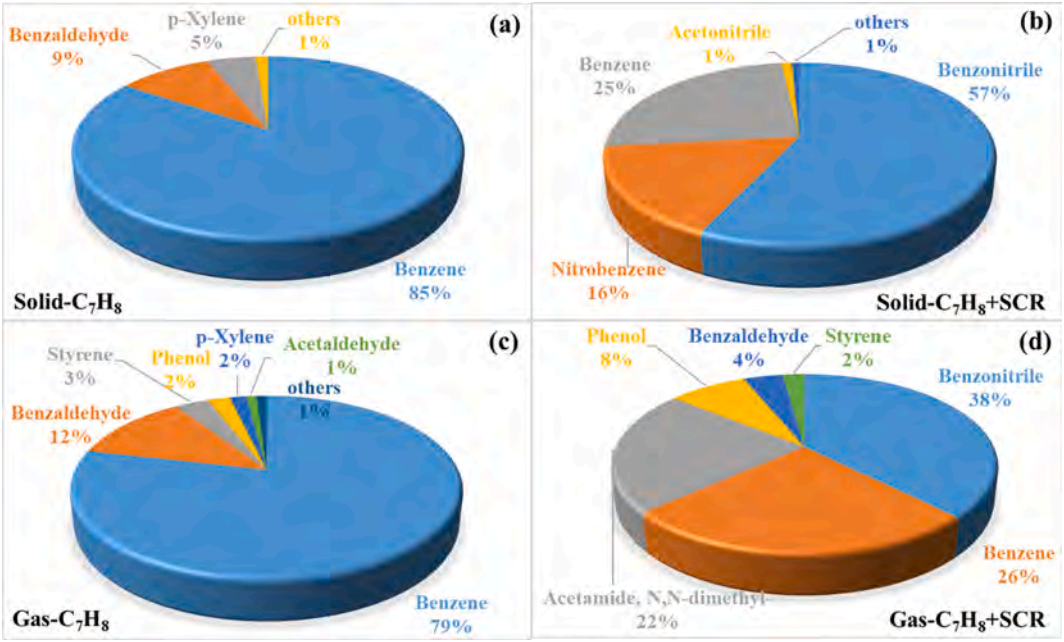

Fig. 5. GC–MS quantitative analyses of (a)-(b) solid byproducts and (c)-(d) gaseous byproducts after reaction at 250 °C.

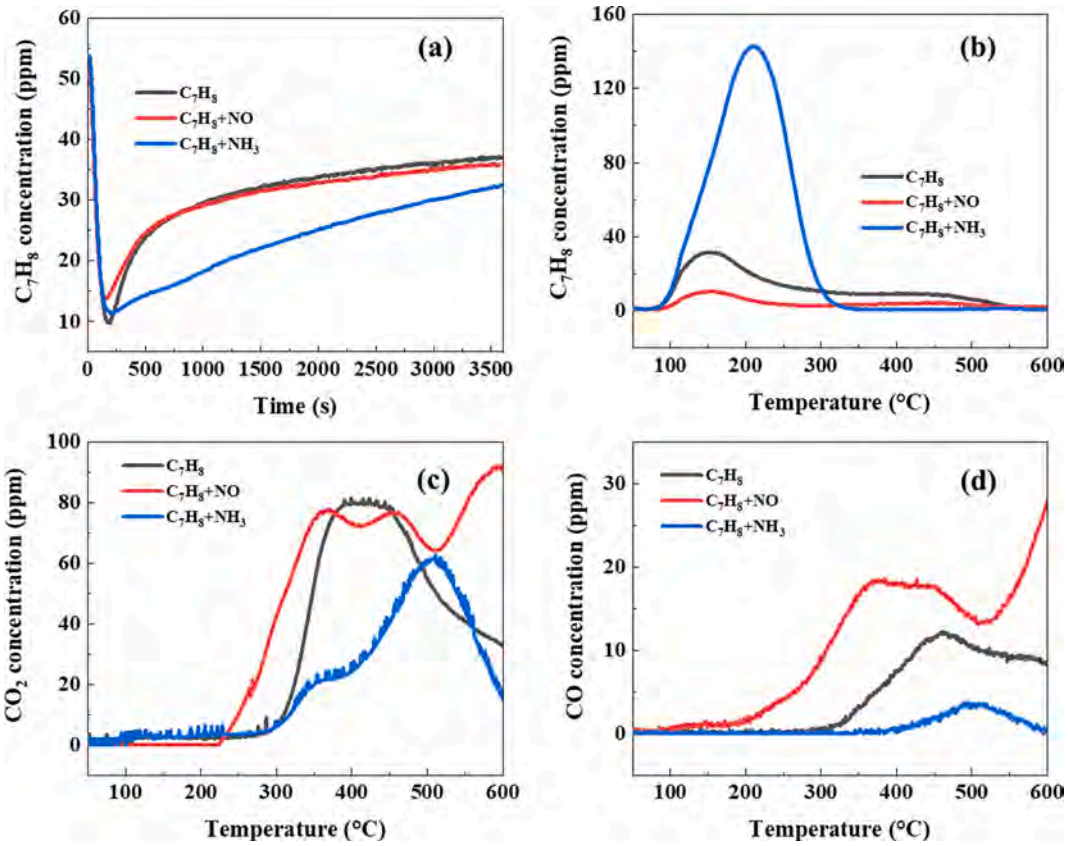

Fig. 6. (a) Adsorption profiles of toluene at 50 °C, (b) C_7H_8-TPD profiles, (c) CO_2 and (d) CO concentrations during C_7H_8-TPD.

toluene catalytic oxidation mechanism has been extensively studied [30,31]. Toluene is firstly adsorbed on catalyst surface and partially oxidized to benzyl alcohol. Then, the benzyl alcohol is oxidized to benzaldehyde and benzoic acid. The benzoic acid is converted to benzene, phenol, benzoquinone, maleate, maleic anhydride step by step. The maleic anhydride is further oxidized to small molecular species such as carbonate, acetic acid and acetaldehyde, and finally mineralized to CO_2 and H_2O [32,33]. When NO and NH_3 were added, several organic nitrogen containing compounds were detected, such as nitriles and nitrobenzene. NH_3 reacted with benzaldehyde to form intermediate PhCH = NH that subsequently dehydrogenated to yield benzonitrile [2]. Byproducts acetic acid or acetaldehyde reacted with gaseous NH_3 through nucleophilic addition and dehydration to generate acetonitrile [1]. The nitrobenzene may be generated from the oxidation of benzenamine that was formed by the reaction between byproduct phenol and gaseous NH_3.

More oxygen containing compounds were identified in the gaseous byproducts of individual toluene oxidation by GC–MS (Fig. S3b and Table S2), such as acetaldehyde, acetone, and phenol. Benzonitrile also existed in the gaseous byproducts, but its amount was significantly smaller than that in solid byproducts. As summarized in Fig. 5a, c, benzene and benzaldehyde were the major components both in solid (94%) and gaseous (91%) byproducts after individual toluene oxidation at 250 °C. Small molecular oxygen containing compounds (e.g., acetone and acetaldehyde) tended to present in gas. The proportions of nitrogen containing compounds reached 74% in solid byproducts and 60% in gaseous byproducts after the addition of NO and NH_3 (Fig. 5b, d). At the same time, the proportions of benzaldehyde in solid and gaseous byproducts decreased from 9% and 12% to 0.6% and 4%, respectively. The proportion of acetaldehyde in gaseous byproducts also decreased from 1% to zero. It can be concluded that NH_3 and NO are prone to reacting with byproduct aldehydes to generate poisoned byproduct nitriles in simultaneous removal of toluene and NO.

Table 2
Quantitative analysis of TPD results (μmol/g).

TPD	C_7H_{8ads}	C_7H_{8des}	CO_2	CO
C_7H_8	106.2	54.3	158.1	22.6
C_7H_8 + NO	104.1	17.2	207.0	49.3
C_7H_8 + NH_3	160.7	143.0	90.3	3.5

3.4. Mechanism investigation

3.4.1. Adsorption-desorption behavior

The adsorption–desorption behaviors of reactants were investigated by TPD (C_7H_8-TPD, C_7H_8 + NH_3-TPD and C_7H_8 + NO-TPD). The adsorption amount of toluene in C_7H_8-TPD was 106.2 μmol/g (Fig. 6a and Table 2). NO slightly decreased the adsorption of toluene to 104.1 μmol/g. The NO adsorption was also inhibited by toluene [11]. The competitive adsorption between NO and C_7H_8 was identified. As for the desorption behavior (Fig. 6b-d), NO decreased the desorption amount of toluene from 54.3 μmol/g to 17.2 μmol/g. However, the desorption amounts of CO_2 and CO increased from 158.1 μmol/g and 22.6 μmol/g to 207.0 μmol/g and 49.3 μmol/g, respectively. The initial temperatures of CO_2 and CO production were 222 °C and 82 °C accordingly, which were significantly lower than that in C_7H_8-TPD (277 °C and 276 °C). The temperatures corresponding to the maximum CO_2 and CO concentrations possessed a similar tendency. These results indicated that NO promoted the light-off and the mineralization of toluene during desorption process. NO could be oxidized to NO_2 when temperature raised [10,11]. NO_2 was a strong oxidizer that accelerated toluene oxidation.

Different from NO, NH_3 increased the adsorption and desorption amounts of toluene to 160.7 μmol/g and 143.0 μmol/g. Zhao et al. [19] found abundant Brønsted acid sites were beneficial for toluene

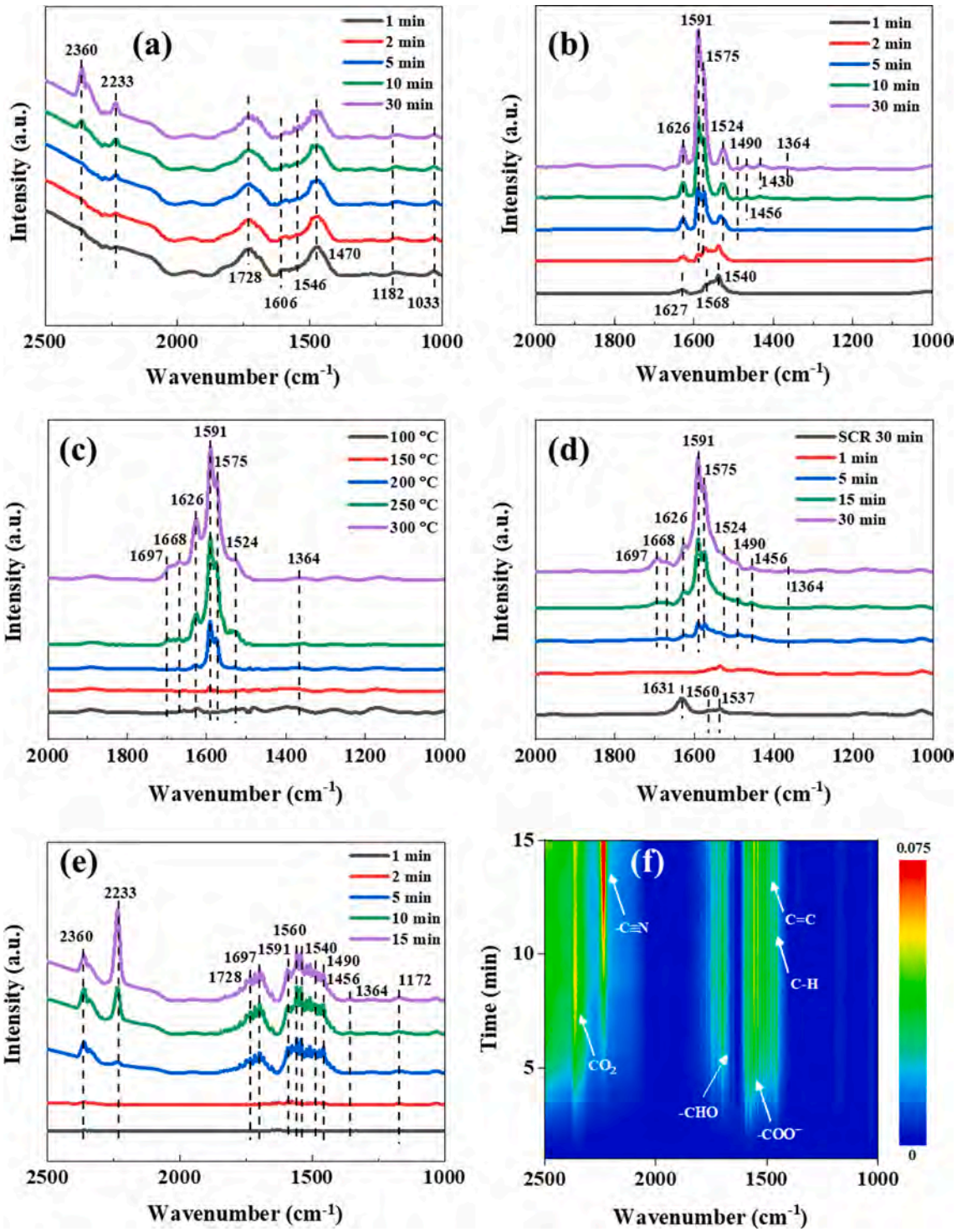

Fig. 7. *In situ* DRIFTs spectra recorded of (a) toluene adsorption on NH_3 pre-adsorbed catalyst at 250 °C, (b) toluene adsorption on NO pre-adsorbed catalyst at 250 °C, (c) toluene oxidation, (d) toluene oxidation at 250 °C on NH_3-SCR pre-reacted catalyst, (e) and (f) toluene oxidation in the presence of NO and NH_3 at 250 °C.

adsorption. In a theory proposed by Li et al. [5], the dissociated free H atoms from NH_{3ads} were captured by the catalyst surface and converted into Brønsted acid sites ($NH_{3ads} + O \rightarrow -NH_{2ads}$ + Brønsted). The additional Brønsted acid sites provided by NH_3 may promote the toluene adsorption. But the CO_2 and CO desorption amounts decreased to 90.3 μmol/g and 3.5 μmol/g, respectively. The initial temperature of CO_2 production (277 °C) was the same as C_7H_8-TPD. Whereas, the initial temperature of CO production (380 °C) was higher. At the same time, the temperatures corresponding to the maximum CO_2 and CO concentrations (508 and 506 °C) were much higher than that in C_7H_8-TPD (398 and 461 °C). NH_3 was competitively oxidized with toluene by active oxygen on catalyst surface [16]. NH_3 could also react with toluene to form byproducts (e.g., nitriles) as described in Section 3.3. Hence, the light-off and deep oxidation of toluene were restricted in the presence of NH_3.

3.4.2. *In-situ DRIFTs analysis*

The adsorption species were subsequently characterized by *in-situ*

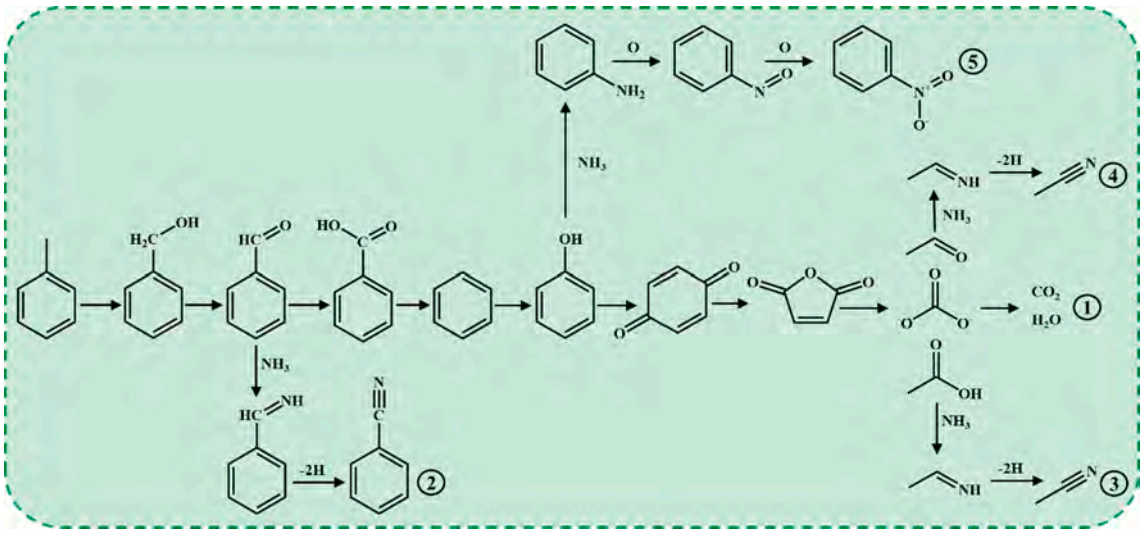

Fig. 8. Toluene catalytic oxidation mechanism and proposed formation routes of nitrogen containing compounds at 250 °C.

DRIFTs. As shown in Fig. 7a, there were six bands observed when NH_3 was adsorbed. The bands at 1728, 1606, 1470, 1182 and 1033 cm^{-1} were assigned to the coordinated NH_3 on the L acid sites [7,34]. The band at 1546 cm^{-1} was related to the ionic NH_4^+ on B acid sites [34]. When toluene passed the NH_3-pretreated catalyst, the bands at 1200–2000 cm^{-1} were overlapped by NH_3 adsorption species. The band at 2360 cm^{-1} belonged to the stretching vibrations of C—O bonds from CO_2 [16]. Similar with our previous findings [10,11], the nitrile species (e.g., acetonitrile and benzonitrile) at 2233 cm^{-1} were identified, which was consistent with the results of byproduct identification. There were three bands observed when NO was adsorbed (Fig. 7b). The band at 1627 cm^{-1} was assigned to adsorbed NO_2 species. The bands at 1568 and 1540 cm^{-1} were ascribed to bidentate nitrates [1]. When toluene passed the NO-pretreated catalyst, several bands appeared. The band at 1490 cm^{-1} was related to the stretching vibration of C═C in aromatic ring [35]. The bands at 1456 and 1364 cm^{-1} were assigned to the bending vibration of C—H in methylene group and methyl group [36], respectively. The band at 1591 cm^{-1} belonged to the stretching vibration of —COO^- in carboxylate [35]. The bands at 1575 and 1524 cm^{-1} were ascribed to the stretching vibration of —COO^- in carbonate [37]. Moreover, the band at 1626 cm^{-1} was recognized as the bending vibration of H—O—H in water [36].

The DRIFTs spectra of toluene oxidation without/with NO and NH_3 were shown in Fig. 7c-f. The bands at 1697 and 1668 cm^{-1} were recognized as the stretching vibration of C═O in aldehyde group [38], which was more obvious at temperatures higher than 250 °C (Fig. 7c). Benzaldehyde was identified both in the solid and gaseous byproducts (Table S1 and S2). When toluene was oxidized on NH_3-SCR pre-reacted catalyst, the initial bands disappeared quickly (Fig. 7d). Comparing with Fig. 7c, the band intensity for water (1626 cm^{-1}) was slightly decreased. Less toluene was completely oxidized when NO and NH_3 were present. Furthermore, when toluene was oxidized in the presence of NO and NH_3 (Fig. 7e, f), a distinct C≡N band in nitriles was observed. The C═C in benzene ring and C—H in methyl group were more pronounced. Instead, the intensities of C═O in aldehyde group (1668 cm^{-1}), —COO^- in carboxylate or carbonate (1591, 1575 and 1524 cm^{-1}) and H—O—H in water (1626 cm^{-1}) were less significant compared with individual toluene oxidation (Fig. 7c). These results demonstrated that NO and NH_3 inhibited the deep oxidation of toluene.

3.4.3. *Reaction mechanism*

Based on aforementioned results, the toluene catalytic oxidation mechanism was summarized in Fig. 8. At 250 °C, the toluene oxidation followed a MvK mechanism [39,40] (**Path 1**). Toluene was firstly adsorbed on catalyst surface and oxidized to benzyl alcohol, generating reduced metal oxides at the same time. The benzyl alcohol was further oxidized to benzaldehyde, benzoic acid, benzene, phenol and benzoquinone. Then the benzoquinone underwent ring opening reaction to form maleic anhydride species, carbonate and acetic acid. Finally, the small molecular species were mineralized to CO_2 and H_2O. The lattice oxygen was continuously replenished by gaseous O_2 and the reduced metal oxides were oxidized to accomplish a redox cycle.

The addition of SCR reactants (NO and NH_3) enhanced the toluene conversion, but decreased the CO_2 selectivity, which indicated more byproducts were generated. Benzonitrile was the dominant organic nitrogen containing compound generated by the reaction of intermediate benzaldehyde and NH_3 (**Path 2**). Intermediates acetic acid and acetaldehyde could react with NH_3 to form trace amount of acetonitrile (**Path 3 and Path 4**). Intermediate phenol may react with NH_3 to form benzenamine that subsequently oxidized to nitrobenzene (**Path 5**). These nitrogen containing compounds were mainly observed in the solid byproducts deposited on catalyst surface, which deactivated the catalyst. The **paths 2–5** consumed the toluene oxidation intermediates, resulting in a higher toluene conversion and less mineralization products (CO_2 and H_2O).

4. Conclusions

The simultaneous removal of toluene and NO was investigated over a MnCe/HZSM-5 catalyst. Although NH_3-SCR reactants (NO and NH_3) increased the toluene conversion at 250 °C, more byproducts were generated and the CO_2 selectivity decreased. The effects of NO and NH_3 on toluene oxidation included (1) accelerating the decrease of Mn^{4+}, Ce^{3+}, O_{sur} proportions and L acid sites, (2) competitive adsorption between NO and toluene, (3) promotion of toluene oxidation by NO and inhibition of toluene oxidation by NH_3, (4) reaction with intermediates (e.g., aldehydes and phenol) to form organic nitrogen containing compounds (e.g., nitriles and nitrobenzene) that transformed more carbon into byproducts and deactivated the catalyst.

CRediT authorship contribution statement

Peng Lu: Conceptualization, Investigation, Methodology, Writing – original draft. **Lyumeng Ye:** Methodology, Validation. **Xianhui Yan:** Investigation, Methodology. **Dingsheng Chen:** Resources. **Dongyao Chen:** Resources. **Xiongbo Chen:** Resources. **Ping Fang:** Resources. **Chaoping Cen:** Supervision, Funding acquisition, Methodology.

Declaration of Competing Interest

The authors declare that they have no known competing financial interests or personal relationships that could have appeared to influence the work reported in this paper.

Acknowledgement

This work was supported by the National Key Research and Development Plan of China (2019YFC0214300, 2020YFF0408886), the Central Public-interest Scientific Institution Basal Research Fund of China (PM-zx703-202104-059, PM-zx703-202104-087) and the Project of Science and Technology Program of Guangzhou, China (202102020135).

Appendix A. Supplementary material

Supplementary data to this article can be found online at https://doi.org/10.1016/j.apsusc.2021.150836.

References

[1] L. Ye, P. Lu, Y. Peng, J. Li, H. Huang, Impact of NO_x and NH_3 addition on toluene oxidation over MnO_x-CeO_2 catalyst, J. Hazard. Mater. 416 (2021) 125939.
[2] W. Jiang, Y. Yu, F. Bi, P. Sun, X. Weng, Z. Wu, Synergistic elimination of NO_x and chloroaromatics on a commercial V_2O_5-WO_3/TiO_2 catalyst: Byproduct analyses and the SO_2 effect, Environ. Sci. Technol. 53 (2019) 12657–12667.
[3] X. Huang, D. Wang, Q. Yang, Y. Peng, J. Li, Multi-pollutant control (MPC) of NO and chlorobenzene from industrial furnaces using a vanadia-based SCR catalyst, Appl. Catal., B 285 (2021) 119835.
[4] M. Gallastegi-Villa, A. Aranzabal, J.A. González-Marcos, J.R. González-Velasco, Metal-loaded ZSM5 zeolites for catalytic purification of dioxin/furans and NO_x containing exhaust gases from MWI plants: Effect of different metal cations, Appl. Catal., B 184 (2016) 238–245.
[5] G. Li, K. Shen, L. Wang, Y. Zhang, H. Yang, P. Wu, B. Wang, S. Zhang, Synergistic degradation mechanism of chlorobenzene and NO over the multi-active center catalyst: The role of NO_2, Brønsted acidic site, oxygen vacancy, Appl. Catal., B 286 (2021) 119865.
[6] D. Wang, Q. Chen, X. Zhang, C. Gao, B. Wang, X. Huang, Y. Peng, J. Li, C. Lu, J. Crittenden, Multipollutant control (MPC) of flue gas from stationary sources using SCR technology: A critical review, Environ. Sci. Technol. 55 (2021) 2743–2766.
[7] L. Ye, P. Lu, X. Chen, P. Fang, Y. Peng, J. Li, H. Huang, The deactivation mechanism of toluene on MnO_x-CeO_2 SCR catalyst, Appl. Catal., B 277 (2020) 119257.
[8] E. Japke, M. Casapu, V. Trouillet, O. Deutschmann, J.D. Grunwaldt, Soot and hydrocarbon oxidation over vanadia-based SCR catalysts, Catal. Today 258 (2015) 461–469.
[9] L. Gan, W. Shi, K. Li, J. Chen, Y. Peng, J. Li, Synergistic Promotion Effect between NO_x and Chlorobenzene Removal on MnO_x-CeO_2 Catalyst, ACS Appl. Mater. Interfaces 10 (2018) 30426–30432.
[10] P. Lu, L. Ye, X. Yan, X. Chen, P. Fang, D. Chen, D. Chen, C. Cen, N_2O inhibition by toluene over Mn-Fe spinel SCR catalyst, J. Hazard. Mater. 414 (2021) 125468.
[11] P. Lu, L. Ye, X. Yan, P. Fang, X. Chen, D. Chen, C. Cen, Impact of toluene poisoning on MnCe/HZSM-5 SCR catalyst, Chem. Eng. J. 414 (2021) 128838.
[12] X.u. Huang, Z. Liu, D. Wang, Y. Peng, J. Li, The effect of additives and intermediates on vanadia-based catalyst for multi-pollutant control, Catal. Sci. Technol. 10 (2020) 323–326.
[13] F. Martinovic, F. Deorsola, M. Armandi, B. Bonelli, R. Palkovits, S. Bensaid, R. Pirone, Composite Cu-SSZ-13 and CeO_2-SnO_2 for enhanced NH_3-SCR resistance towards hydrocarbon deactivation, Appl. Catal., B 282 (2021) 119536.
[14] Q. Wang, P.C. Hung, S. Lu, M.B. Chang, Catalytic decomposition of gaseous PCDD/Fs over V_2O_5/TiO_2-CNTs catalyst: Effect of NO and NH_3 addition, Chemosphere 159 (2016) 132–137.
[15] D. Wang, J. Chen, Y. Peng, W. Si, X. Li, B. Li, J. Li, Dechlorination of chlorobenzene on vanadium-based catalysts for low-temperature SCR, Chem. Commun. 54 (2018) 2032–2035.
[16] L. Zhao, Y. Huang, J. Zhang, L. Jiang, Y. Wang, Al_2O_3-modified CuO-CeO_2 catalyst for simultaneous removal of NO and toluene at wide temperature range, Chem. Eng. J. 397 (2020) 125419.
[17] C. Zhang, Y. Wang, G. Li, L. Chen, Q. Zhang, D. Wang, X. Li, Z. Wang, Tuning smaller Co_3O_4 nanoparticles onto HZSM-5 zeolite via complexing agents for boosting toluene oxidation performance, Appl. Surf. Sci. 532 (2020) 147320.
[18] X. Zhang, F. Bi, Z. Zhu, Y. Yang, S. Zhao, J. Chen, X. Lv, Y. Wang, J. Xu, N. Liu, The promoting effect of H_2O on rod-like $MnCeO_x$ derived from MOFs for toluene oxidation: A combined experimental and theoretical investigation, Appl. Catal., B 297 (2021) 120393.
[19] X. Zhang, Y. Yang, Q. Zhu, M. Ma, Z. Jiang, X. Liao, C. He, Unraveling the effects of potassium incorporation routes and positions on toluene oxidation over α-MnO_2 nanorods: Based on experimental and density functional theory (DFT) studies, J. Colloid Interface Sci. 598 (2021) 324–338.
[20] X. Weng, P. Sun, Y. Long, Q. Meng, Z. Wu, Catalytic Oxidation of Chlorobenzene over $Mn_xCe_{1-x}O_2$/HZSM-5 Catalysts: A Study with Practical Implications, Environ. Sci. Technol. 51 (2017) 8057–8066.
[21] G. Carja, Y. Kameshima, K. Okada, C.D. Madhusoodana, Mn–Ce/ZSM5 as a new superior catalyst for NO reduction with NH_3, Appl. Catal., B 73 (2007) 60–64.
[22] R. Yan, S. Lin, Y. Li, W. Liu, Y. Mi, C. Tang, L. Wang, P. Wu, H. Peng, Novel shielding and synergy effects of Mn-Ce oxides confined in mesoporous zeolite for low temperature selective catalytic reduction of NO_x with enhanced SO_2/H_2O tolerance, J. Hazard. Mater. 396 (2020) 122592.
[23] C.A. Emeis, Determination of integrated molar extinction coefficients for infrared absorption bands of pyridine adsorbed on solid acid catalysts, J. Catal. 141 (1993) 347–354.
[24] T. Yashima, N. Hara, Infrared study of cation-exchanged mordenites and Y faujasites adsorbed with ammonia and pyridine, J. Catal. 27 (1972) 329–333.
[25] B. de Rivas, R. López-Fonseca, J.R. González-Velasco, J.I. Gutiérrez-Ortiz, On the mechanism of the catalytic destruction of 1,2-dichloroethane over Ce/Zr mixed oxide catalysts, J. Mol. Catal. A: Chem. 278 (2007) 181–188.
[26] H. Wang, B. Peng, R. Zhang, H. Chen, Y. Wei, Synergies of Mn oxidative ability and ZSM-5 acidity for 1, 2-dichloroethane catalytic elimination, Appl. Catal., B 276 (2020) 118922.
[27] F. Bi, X. Zhang, Q. Du, K. Yue, R. Wang, F. Li, N. Liu, Y. Huang, Influence of pretreatment conditions on low-temperature CO oxidation over Pd supported UiO-66 catalysts, Mol. Catal. 509 (2021) 111633.
[28] K. Zeng, Y. Wang, C. Huang, H. Liu, X. Liu, Z. Wang, J. Yu, C. Zhang, Catalytic Combustion of Propane over $MnNbO_x$ Composite Oxides: The Promotional Role of Niobium, Ind. Eng. Chem. Res. 60 (2021) 6111–6120.
[29] K. Zeng, Z. Wang, D. Wang, C. Wang, J. Yu, G. Wu, Q. Zhang, X. Li, C. Zhang, X. S. Zhao, Three-dimensionally ordered macroporous $MnSmO_x$ composite oxides for propane combustion: Modification effect of Sm dopant, Catal. Today 376 (2021) 211–221.
[30] X. Chen, X. Chen, E. Yu, S. Cai, H. Jia, J. Chen, P. Liang, In situ pyrolysis of Ce-MOF to prepare CeO_2 catalyst with obviously improved catalytic performance for toluene combustion, Chem. Eng. J. 344 (2018) 469–479.
[31] C. He, J. Cheng, X. Zhang, M. Douthwaite, S. Pattisson, Z. Hao, Recent advances in the catalytic oxidation of volatile organic compounds: A review based on pollutant sorts and sources, Chem. Rev. 119 (2019) 4471–4568.
[32] W. Yang, Z.A. Su, Z. Xu, W. Yang, Y. Peng, J. Li, Comparative study of α-, β-, γ- and δ-MnO_2 on toluene oxidation: Oxygen vacancies and reaction intermediates, Appl. Catal., B 260 (2020) 118150.
[33] J. Zhong, Y. Zeng, D. Chen, S. Mo, M. Zhang, M. Fu, J. Wu, Z. Su, P. Chen, D. Ye, Toluene oxidation over Co^{3+}-rich spinel Co_3O_4: Evaluation of chemical and by-product species identified by in situ DRIFTS combined with PTR-TOF-MS, J. Hazard. Mater. 386 (2020) 121957.
[34] S. Xiong, J. Chen, N. Huang, T. Yan, Y. Peng, J. Li, The poisoning mechanism of gaseous HCl on low-temperature SCR catalysts: MnO_x-CeO_2 as an example, Appl. Catal., B 267 (2020) 118668.
[35] L. Zhao, Z. Zhang, Y. Li, X. Leng, T. Zhang, F. Yuan, X. Niu, Y. Zhu, Synthesis of Ce_aMnO_x hollow microsphere with hierarchical structure and its excellent catalytic performance for toluene combustion, Appl. Catal., B 245 (2019) 502–512.
[36] Z. Su, W. Yang, C. Wang, S. Xiong, X. Cao, Y. Peng, W. Si, Y. Weng, M. Xue, J. Li, Roles of oxygen vacancies in the bulk and surface of CeO_2 for toluene catalytic combustion, Environ. Sci. Technol. 54 (2020) 12684–12692.
[37] X. Chen, X. Chen, S. Cai, E. Yu, J. Chen, H. Jia, MnO_x/Cr_2O_3 composites prepared by pyrolysis of Cr-MOF precursors containing in situ assembly of MnO_x as high stable catalyst for toluene oxidation, Appl. Surf. Sci. 475 (2019) 312–324.
[38] Z. Hou, X. Zhou, T. Lin, Y. Chen, X. Lai, J. Feng, M. Sun, The promotion effect of tungsten on monolith Pt/$Ce_{0.65}Zr_{0.35}O_2$ catalysts for the catalytic oxidation of toluene, New J. Chem. 43 (2019) 5719–5726.
[39] J.-R. Li, W.-P. Zhang, C. Li, H. Xiao, C. He, Insight into the catalytic performance and reaction routes for toluene total oxidation over facilely prepared Mn-Cu bimetallic oxide catalysts, Appl. Surf. Sci. 550 (2021) 149179.
[40] P. Liu, Y. Liao, J. Li, L. Chen, M. Fu, P. Wu, R. Zhu, X. Liang, T. Wu, D. Ye, Insight into the effect of manganese substitution on mesoporous hollow spinel cobalt oxides for catalytic oxidation of toluene, J. Colloid Interface Sci. 594 (2021) 713–726.